Bioorganic Chemistry 82 (2019) 241–245

Contents lists available at ScienceDirect

Bioorganic Chemistry

journal homepage: www.elsevier.com/locate/bioorg

In vitro biological evaluation and molecular docking studies of natural and semisynthetic flavones from *Gardenia oudiepe* (Rubiaceae) as tyrosinase inhibitors

M.D. Santi[a,b], C. Bouzidi[c], N.S. Gorod[d], M. Puiatti[d], S. Michel[c], R. Grougnet[c], M.G. Ortega[a,b,*]

[a] *Farmacognosia, Departamento de Ciencias Farmacéuticas, Facultad de Ciencias Químicas, Universidad Nacional de Córdoba, Ciudad Universitaria, Haya de la torre y Medina Allende, Edificio Ciencias II, X5000HUA Córdoba, Argentina*

[b] *Instituto Multidisciplinario de Biología Vegetal (IMBIV-CONICET), Ciudad Universitaria, X5000HUA Córdoba, Argentina*

[c] *Laboratoire de Pharmacognosie, UMR/CNRS 8638, Faculté des Sciences Pharmaceutiques et Biologiques, Université Paris Descartes, Sorbonne Paris Cité, 4, Avenue de l'Observatoire, 75006 Paris, France*

[d] *Instituto de Investigaciones en Físico-Química de Córdoba (INFIQC), Departamento de Química Orgánica, Facultad de Ciencias Químicas, Universidad Nacional de Córdoba, Ciudad Universitaria, Haya de la torre y Medina Allende, Edificio Ciencias II, X5000HUA Córdoba, Argentina*

A R T I C L E I N F O

Keywords:
Gardenia oudiepe
Polymethoxylated flavones
Tyrosinase inhibitory activity
Structure-activity relationships
Molecular docking

A B S T R A C T

Hyperpigmentation disorders are difficult to treat without causing permanent depigmentation or irritation. The most effective hypopigmenting agents are tyrosinase inhibitors, however some of those currently used have shown serious side effects. As several classes of flavonoids have already demonstrated ability to inhibit tyrosinase, a library of natural polymethoxyflavones isolated (**1–7**) from the bud exudate of *Gardenia oudiepe* and semi-synthetic derivatives (**8**,**9**) were evaluated. IC_{50} of the most active compounds were in the micromolar range. The strongest inhibitors **1**, **2** and **3** all shared a 3′,4′-dimethoxy-5′-hydroxy trisubstituted B ring. These SAR conclusions were confirmed by molecular docking studies. The mode of interaction with the enzyme was elucidated, and important interactions between the most active compounds and catalytic residues of tyrosinase were observed. All of these data provided a library of compounds as potential leaders for the design of new depigmenting agents and formulations.

1. Introduction

Melanin biosynthesis is one of the most important factors in mammal skin color determination. This pigment protects against UV radiation, preventing mutations in cellular DNA, which could cause abnormal conformations in the expression of DNA [1–5]. An overproduction of melanin leads to hyperpigmentary disorders, such as lentigo, ephelides, nevus and other skin diseases. These pathologies result in devastating conditions for many patients, strongly impacting the quality of life [6–8]. Besides, agents currently used to reduce for hyperpigmentation, such as hydroquinone or kojic acid, have undesirable effects such as carcinogenesis, hepatotoxicity, dermatitis [9,10]. Tyrosinase is responsible for the first two steps on melanin synthesis, and could be thus considered as a key-enzyme in the melanogenic cascade [9,11,12]. Flavonoids show a high potential for tyrosinase inhibition [6,11–20] and may be an important source of depigmenting agents. We have recently reported the ability of nine polymethoxyflavones (PMF) isolated and semi-synthetized from the bud exudate of *Gardenia oudiepe* Vieill. (syn. *G. cerifera* S. Moore) to inhibit xanthine oxidase [21]. The potentiality of these compounds to interact in active sites of enzymes drove us to evaluate their monophenolase mushroom tyrosinase inhibitory activity, in order to establish some structure-activity relationships and to elucidate a plausible binding mode through molecular docking studies.

2. Results and discussion

2.1. In vitro tyrosinase inhibitory activity

Nine flavones were evaluated for monophenolase tyrosinase inhibitory activity. **1–7** were natural products isolated from the bud exudate of *G. oudiepe*, **8** and **9** were hemisynthetized from **6** and **7**, respectively (Table 1). **1–9** were evaluated at several concentrations on mushroom tyrosinase enzyme, using L-tyrosine as substrate and kojic

* Corresponding author at: Farmacognosia, Departamento de Ciencias Farmacéuticas, Facultad de Ciencias Químicas, Universidad Nacional de Córdoba, Ciudad Universitaria, Haya de la torre y Medina Allende, Edificio Ciencias II, X5000HUA Córdoba, Argentina.
E-mail address: gortega@fcq.unc.edu.ar (M.G. Ortega).

https://doi.org/10.1016/j.bioorg.2018.10.034
Received 15 March 2018; Received in revised form 13 October 2018; Accepted 17 October 2018
Available online 25 October 2018
0045-2068/

Table 1
Structures and mushroom tyrosinase inhibition of **1–9** compounds.

Substitution pattern	Compound	6	7	3′	4′	5′	IC_{50} (μM)
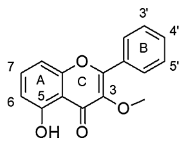	**1**	OCH_3	OH	OCH_3	OCH_3	OH	(6.71 ± 0.001)[#]
	2	H	OH	OCH_3	OCH_3	OH	(13.20 ± 0.06)[#]
	3	H	OCH_3	OCH_3	OCH_3	OH	(17.66 ± 0.001)[#]
	4	OCH_3	OH	OCH_3	OCH_3	OCH_3	(62.68 ± 0.001)[#]
	5	OCH_3	OH	H	OH	H	(73.03 ± 0.22)[#]
	6	H	OH	H	OH	H	(103.56 ± 0.11)[#]
	7	OCH_3	OH	H	OCH_3	H	n.d[*]
	8	H	OCH_3	H	OCH_3	H	n.d[**]
	9	OCH_3	OCH_3	H	OCH_3	H	n.d[***]

Positive control: Kojic acid IC_{50} = (12.12 ± 0.001) μM. Media ± SD of at least 3 determinations.
n.d not determined. Inhibition at 100 μM: nd[*]: (33.9 ± 0.2%), nd[**]: (19.25 ± 1.0%), nd[***]: (7.5 ± 0.7%).
[#] Statistically different respect to kojic acid, $p < 0.001$.

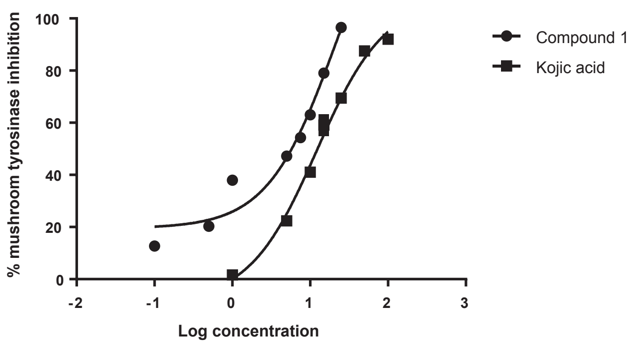

Fig. 1. Concentration-dependent inhibition of mushroom monophenolase tyrosinase activity by compound **1** and kojic acid (positive control) (N = 3).

acid as reference inhibitor. All compounds showed a concentration dependent inhibition. The IC_{50} values for the PMFs which inhibited more than 50% at 100 μM were determined (Table 1).

The natural PMF, compound **1**, was the strongest inhibitor being two folds more active than kojic acid. In Fig. 1 is shown the nonlinear fitting of concentration-response data for compound **1** and the reference positive inhibitor, kojic acid.

2.2. Structure-activity relationships

Reports about the influence of hydroxy and methoxy substitution pattern of flavone core in terms of tyrosinase monophenolase inhibition are limited and controversial [11,22], but all agree with the importance of a hydroxy substituent on C5 and C7.

In this context, this work aimed to determine some structural requirements in order to complete available data.

All compounds shared a structure including a methoxy group on position 3, a hydroxy group on position 5 and oxygenated aromatic carbons in C4′ and C7.

The strongest inhibitors **1**, **2** and **3** possess the same trisubstituted 3′,4′-dimethoxy-5′-hydroxy B ring. Thus, this substitution pattern looks essential for monophenolase inhibition (Table 1).

Compound **1** that bears an additional methoxy group in C6 and a hydroxy group in C7 was the most active, approximately two-fold more than the reference inhibitor, kojic acid (Fig. 1).

With the same B ring, compound **2** with a proton instead of a methoxy group on C6 and compound **3** that differs from **2** by a methoxy instead of a hydroxy on C7 were in the same range of activity as kojic acid.

The importance of the B ring substitution pattern is also highlighted by the fact that with the same 5,7-dihydroxy-6-methoxy A ring than **1**, compounds **4**, **5** and **7** were at least 10-fold less active. This assertion is valid for a less hindered B ring, as in the case of **5** and **7**, or more hindered, such as compound **4**.

When comparing the IC_{50} of **1** *vs* **2** and **5** *vs* **6**, it appears that compounds bearing a methoxy group in position 6 are more active than those which are not substituted on this position. The importance of the presence of an oxygen in C6 had been established for the diphenolase activity of tyrosinase in previous report [19].

Finally, comparison of the IC_{50} values of **2** and **3**, and of the inhibitory activity at 100 μM of **7** and **9**, respectively, allowed to deduce that compounds bearing a hydroxy group on C7 are slightly better inhibitor than those with a methoxy substitution, in agreement with previous studies [11].

2.3. Molecular modeling studies

Tyrosinase (PDB code: 2Y9W) is found as a tetrameric protein composed of two subunits of ~43 kDa (H subunit) and two subunits of ~14 kDa (L subunit), with a molecular mass of 120 kDa. The H subunit is tyrosinase, while the identity, function, and origin of the L subunit are unknown. The active site is composed of a binuclear copper site, with each copper ion coordinated by three histidine residues and it is located at the heart of two pairs of antiparallel α-helices [23].

In order to establish the interactions leading to the observed structure-activity relationships and to understand the differences in the IC_{50} values of the evaluated compounds, molecular modeling studies were carried out. To do so, in the first place molecular docking calculations were used to build 10 different complexes of each flavone with mushroom tyrosinase (PDB code: 2Y9W), the active site for the docking procedure was defined taking into account the informed by Ismaya et al. [23], for the co-crystallized ligand, tropolone. Finally, a short molecular dynamic simulation of each complex followed by an evaluation of the binding energy [24] was performed in order to select the best complex of each PMF with the enzyme (Supplementary Material, Table S1).

It was found that the more stable complexes were formed with the strongest inhibitors **1–3**, with energies values of −31.0, −28.9 and −27.7 kcal/mol, respectively. All these complexes include the B ring toward the binding site (Fig. 2 and Supplementary Material, Fig. S1). On the other side, less stable complexes were found for compounds **4–9**, with energies values of −21.5 to −24.5 kcal/mol (Supplementary Material, Figs. S2–S10).

As described above, **1–3** share a common structural B ring. According to this, it was expected that the B ring should be located at the same place in the complexes of these compounds. This was actually observed as the B ring of **1–3** was close to histidine residues 84, 258, and 262 and the copper atoms in the active site of the enzyme (Fig. 2). Nevertheless, the position of the A and C rings was not the same for **1–3**, indicating that the substitution or the position of the other part of the molecule, that is not bound to the active site, is also important according to the differences observed for their IC_{50} values (Supplementary Material, Fig. S1).

Finally, the analysis of all the structural requirements with the

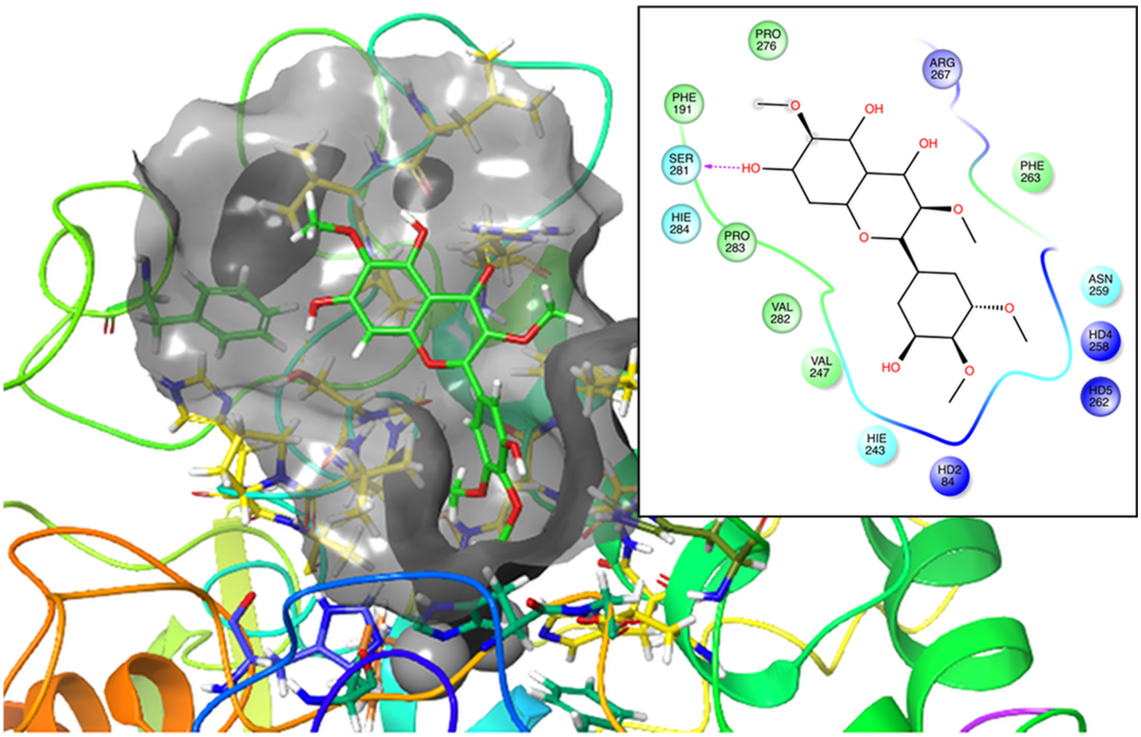

Fig. 2. Best complex between **1** and mushroom tyrosinase. The inset shows the interactions of the ligand with the enzyme. In blue polar interactions with the histidines of the active site, in green hydrophobic interactions and in light blue polar interactions.

molecular modeling results has underlined the importance of the B ring substitution pattern to enhance the tyrosinase inhibitory activity of this library of PMFs. The presence of an hydroxy group in position 5′, and two methoxy groups in positions 3′ and 4′ of the B ring is closely related to the B ring (2′,3′-dimethoxy-4′hydroxy) of the isoflavone haginin A, which exhibited an IC_{50} of 5 µM [25].

When compared to recently published xanthine oxidase inhibitory activity of PMFs [21], IC_{50}, docking data and consequently structure-activity relationships were completely different. Compounds **6** and **5** with a low-hindered 4′-hydroxy-B ring, which showed a weak tyrosinase inhibition, were nanomolar range inhibitors of xanthine oxidase. Thus, despite close structures, PMFs exhibit high level of selectivity towards enzyme target.

3. Conclusion

The monophenolase tyrosinase inhibitory activity of nine PMFs isolated or semisynthetized from *Gardenia oudiepe* was determined. Compounds **1**–**3** with a 3′,4′-dimethoxy-5′-hydroxy B ring were the most potent tyrosinase inhibitors. These data were confirmed by molecular docking studies which showed interactions between the substituents of the B ring with catalytically important histidine residues (84, 258 and 262) located in the active site of the enzyme.

These results suggest that the most active compounds could be candidates for the treatment of pathologies involving tyrosinase, particularly socially problematic hyperpigmentation troubles. Moreover, as the PMFs are isolated from bud exudate, a renewable natural source from a *Gardenia* species easy to cultivate, they may be regarded as new leads for further pharmacomodulation and designing of potent tyrosinase inhibitors, in respect for the environment and sustainable development.

4. Experimental

4.1. Plant material

Aerial parts of *G. oudiepe* including bud exudates were collected in Forêt Plate, North Province of New Caledonia (October 2008). A voucher specimen is available for consultation under the reference POU-0290 (Herbarium of the Botanical and Tropical Ecology Department of the IRD Center, Noumea, New Caledonia).

4.2. Isolation of flavones 1–6 and 9

1L of dichloromethane was used to dissolve 200.0 g of bud exudates of *G. oudiepe*. Filtration through a Büchner funnel followed by evaporation of the solvent under reduced pressure provided 52.0 g of exudates without vegetal inclusions. Several steps of silica gel column chromatographic separations (elution with solvents mixture cyclohexane/dichloromethane and dichloromethane/methanol, increasing polarity) enabled the isolation of flavones **1**–**6** and **9**.

4.3. Semi-synthesis of flavones 7 and 8

Compounds **7** and **8** were obtained by stirring 100 mg of **1** and **4**, respectively, with dimethyl sulfate (Me_2SO_4, 4 equiv.) and 1,8-diazabicyclo[5.4.0]undec-7-en (DBU, 2 equiv.) in dried acetone for 1 h at room temperature. After precipitation and washing of the crudes with iced water, residues were dissolved in 15 mL of ethyl acetate. Then 3 mL of 1 N HCl were added. Extraction with ethyl acetate (3 times, 10 mL each), washing of the organic phase with a saturated NaCl solution, drying over Na_2SO_4, paper filtration, evaporation of the solvent under reduced pressure and purification on silica gel (eluent: dichloromethane/methanol, 95/5, v/v) provided **7** and **8** (yield 69% and 71%, respectively).

NMR data of natural and semi-synthetic PMFs were identical to those previously published (for compounds **1** and **4**–**9** see reference [26]; for compounds **2**–**3** see Ref. [21], the information is also in the SI).

4.4. Tyrosinase inhibition assay

The assay was performed as previously described [14]. Briefly, the medium consisting of 0.25 mL of mushroom tyrosinase solution (200 U/mL), and 0.75 mL of the control solution [Na_3PO_4 buffer (0.1 M, pH 6.8)] or the sample solution [prepared with each flavonoid **1–9** dissolved in DMSO (final concentration 0.1, v/v) and subsequently diluted to the appropriate concentrations with the above buffer] was mixed and preincubated at 25 °C for 10 min. Then, 0.50 mL of L-tyrosine (1.7 mM, Sigma) solution was added. The absorbance was measured at 475 nm after 20 min of incubation. Kojic acid was used as positive control agent. Each treatment was replicated three times. The percent inhibition of tyrosinase activity was calculated as follows: % inhibition = [(Abscontrol × Abssample)/Abscontrol] × 100, where Abscontrol is the absorbance of the control solution and Abssample is the absorbance of the sample solution.

4.5. Calculations and statistics

All assays were independently performed in triplicate, and results were expressed as media ± SD of three separate experiments. The IC_{50} values were estimated using the *GraphPad Prism* 6.0 software on a compatible computer. The results were analyzed by unidirectional analysis of variance (ANOVA) followed by the *Tukey* test for multiple comparisons using *GraphPad Prism* 6.0 software.

4.6. Molecular modeling

The complexes between the ligands and mushroom tyrosinase were obtained by molecular docking with the software VINARDO [27] within the SMINA fork of VINA [28]. The GPU version of Amber14 was used for carrying out molecular dynamics simulations [29,30] and VMD [31] and Maestro [32] were used for the analysis of results and preparation of figures.

The starting coordinates of the protein were taken from Ref. [27], PDB code: 2Y9W. The metal center was parameterized using the tool MCPB.py [33]. Care should be taken when treating copper, since the recommended non-bonded parameters [34] for this metal center did not work properly, and we replaced them by the ones employed by other authors [35–37]. The amberff14SB [38] was employed for the protein residues and the properties of the ligands were obtained by using antechamber [39] with RESP charges [40]. A list with geometries of the ligands is included in the SI.

For the docking two boxes were used, Fig. S11. In a first approximation a big box of (28.0 × 22.5 × 24.0) Å with a grid spacing of 0.325 Å. After these first docking calculations, it was found that the most stable complexes located the inhibitor around the active site, hence a smaller box of (10.0 × 17.0 × 10.0) Å was used to refine the docking search.

After each docking calculation, 9 geometries were obtained and a refinement and recalculation of the binding energy [24] were carried out for each complex to select the best of each ligand. The refinement consist of two 5000 steps of minimization, one with restrictions in the movement of protein atoms, and the other with restrictions in only the residues of the active site (histidines 60, 84, 93, 258, 262 and 295, cysteine 82 and the cooper center) and the ligand. After the minimization the system was solvated with TIP3P water forming an octahedral box, and then 4 ns of molecular simulations were carried out at 300 K, with only one restriction, the position of the atoms of the Cu center. The simulations were carried out within the PME approximation, implemented in the GPU version of Amber14 [28,29]. An average of the binding energy was calculated by selecting 50 snapshots of the last ns of each simulation by using MMPBSA.py [24] tool within a Generalized Born solvation model [41].

Acknowledgments

This work was supported by ANPCyT BID-PICT 1576, CONICET D32/10, SECYT-Universidad Nacional de Cordoba (05/C375), MINCyT Cba PID 2010. M.D.S. is postdoctoral fellows of CONICET. M.G.O. is member of the Research Career of CONICET. Vincent Dumontet and Cyril Poullain are acknowledged for plant collection and identification. The authors also thank the North Province of New Caledonia for permission of field investigations. All calculations were performed with computational resources from the Centro de Computación de Alto Desempeño - Universidad Nacional de Córdoba (http://ccad.unc.edu.ar/), in particular the Mendieta Cluster that belongs to the Facultad de Matemática, Astronomía y Física, that is also part of SNCAD - MinCyT, República Argentina.

Appendix A. Supplementary material

Supplementary data to this article can be found online at https://doi.org/10.1016/j.bioorg.2018.10.034.

References

[1] N. Kollias, R.M. Sayre, L. Zeise, M.R. Chedekel, Photoprotection by melanin, J. Photochem. Photobiol. B 9 (1991) 135–160.
[2] A. Slominski, D.J. Tobin, S. Shibahara, J. Wortsman, Melanin pigmentation in mammalian skin and its hormonal regulation, Physiol. Rev. 84 (2004) 1155–1228.
[3] F.L. Meyskens, P. Farmer Jr, J.P. Fruehauf, Redox regulation in human melanocytes and melanoma, Pigm. Cell Res. 14 (2001) 148–154.
[4] J.M. Pawelek, A.K. Chakraborty, M.P. Osber, S.J. Orlow, K.K. Min, K.E. Rosenzweig, J.L. Bolognia, Molecular cascades in UV-induced melanogenesis: a central role for melanotropins? Pigm. Cell Res. 5 (1992) 348–356.
[5] Y.J. Kim, H. Uyama, Tyrosinase inhibitors from natural and synthetic sources: structure, inhibition mechanism and perspective for the future, Cell. Mol. Life Sci. 62 (2005) 1707–1723.
[6] E.T. Arung, K. Shimizu, H. Tanaka, R. Kondo, 3-Prenyl luteolin, a new prenylated flavone with melanin biosynthesis inhibitory activity from wood of *Artocarpus heterophyllus*, Fitoterapia 81 (2010) 640–643.
[7] P.E. Grimes, Management of hyperpigmentation in darker racial ethnic groups, Semin. Cutan. Med. Surg. 28 (2009) 77–85.
[8] S. Briganti, E. Camera, M. Picardo, Chemical and instrumental approaches to treat hyperpigmentation, Pigm. Cell Res. 16 (2003) 101–110.
[9] S.Y. Seo, V.K. Sharma, N. Sharma, Mushroom tyrosinase: recent prospects, J. Agric. Food Chem. 51 (2003) 2837–2853.
[10] M.D. Njoo, W. Westerhof, J.D. Bos, P.M. Bossuyt, The development of guidelines for the treatment of vitiligo, Arch. Dermatol. 135 (1999) 1514–1521.
[11] T.S. Chang, An updated review of tyrosinase inhibitors, Int. J. Mol. Sci 10 (2009) 2440–2475.
[12] C. Chen, L. Lin, W. Yang, J. Bordon, H.D. Wang, An updated organic classification of tyrosinase inhibitors on melanin biosynthesis, Curr. Org. Chem. 19 (2015) 4–18.
[13] K.T. Cheng, F.L. Hsu, S.H. Chen, P.K. Hsieh, H.S. Huang, C.K. Lee, M.H. Lee, New constituent from *Podocarpus macrophyllus* var. *macrophyllus* shows anti-tyrosinase effect and regulates tyrosinase-related proteins and mRNA in human epidermal melanocytes, Chem. Pharm. Bull. 55 (2007) 757–761.
[14] M.A. Peralta, M.D. Santi, A.M. Agnese, J.L. Cabrera, M.G. Ortega, Flavanoids from *Dalea elegans*: chemical reassignment and determination of kinetics parameters related to their anti-tyrosinase activity, Phytochem. Lett. 10 (2014) 260–267.
[15] M.D. Santi, M.A. Peralta, C.S. Mendoza, J.L. Cabrera, M.G. Ortega, Chemical and bioactivity of flavanones obtained from roots of *Dalea pazensis* Rusby, Bioorg. Med. Chem. Lett. 27 (2017) 1789–1794.
[16] I. Kubo, I. Kinst-Hori, S.K. Chaudhuri, Y. Kubo, Y. Sánchez, T. Ogura, Flavonols from *Heterotheca inuloides*: tyrosinase inhibitory activity and structural criteria, Bioorgan. Med. Chem. 8 (2000) 1749–1755.
[17] H. Gao, J. Nishida, S. Saito, J. Kawabata, Inhibitory effects of 5,6,7-trihydroxyflavones on tyrosinase, Molecules 12 (2007) 86–97.
[18] Y.B. Ryu, T.J. Ha, M.J. Curtis-Long, H.W. Ryu, S.W. Gal, K.H. Park, Inhibitory effects on mushroom tyrosinase by flavones from the stem barks of *Morus lhou* (S.) Koidz, J. Enzyme Inhib. Med. Chem. 23 (2008) 922–930.
[19] M. Singh, M. Kaur, O. Silakari, Flavones: an important scaffold for medicinal chemistry, Eur. J. Med. Chem. 84 (2014) 206–239.
[20] N. Yoshizaki, R. Hashizume, H. Masaki, A polymethoxyflavone mixture extracted from orange peels, mainly containing nobiletin, 3,3′,4′,5,6,7,8-heptamethoxyflavone and tangeretin, suppresses melanogenesis through the acidification of cell organelles, including melanosomes, J. Dermatol. Sci. 88 (2017) 78–84.
[21] M.D. Santi, M. Paulino Zunini, B. Vera, C. Bouzidi, V. Dumontet, A. Abin-Carriquiry, R. Grougnet, M.G. Ortega, Xanthine oxidase inhibitory activity of natural and hemisynthetic flavonoids from *Gardenia oudiepe* (Rubiaceae) in vitro and molecular docking studies, Eur. J. Med. Chem. 143 (2017) 577–582.
[22] F. Solano, S. Briganti, M. Picardo, G. Ghanem, Hypopigmentating agents: an updated review on biological, chemical and clinical aspects, Pigm. Cell Res. 19 (2006) 550–571.
[23] W.T. Ismaya, H.J. Rozeboom, A. Weijn, J.J. Mes, F. Fusetti, H.J. Wichers, B.W. Dijkstra, Crystal structure of *Agaricus bisporus* mushroom tyrosinase: identity of the tetramer subunits and interaction with tropolone, Biochemistry 50 (2011) 5477–5486.

[24] B.R. Miller III, T.D. McGee Jr., J.M. Swails, N. Homeyer, H. Gohlke, A.E.J. Roitberg, MMPBSA.py: an efficient program for end-state free energy calculations, Chem. Theory Comput. 9 (2012) 3314–3321.

[25] J.H. Kim, S.H. Baek, D.H. Kim, T.Y. Choi, T.J. Yoon, J.S. Hwang, M.R. Kim, H.J. Kwon, C.H. Lee, Downregulation of melanin synthesis by haginin a and its application to in vivo lightening model, J. Invest. Dermatol. 128 (2008) 1227–1235.

[26] L.H. Mai, G.G. Chabot, P. Grellier, L. Quentin, V. Dumontet, C. Poulain, L.S. Espindola, S. Michel, H.T.B. Vo, B. Deguin, R. Grougnet, Antivascular and antiparasite activities of natural and hemisynthetic flavonoids from New Caledonian *Gardenia* species (Rubiaceae), Eur. J. Med. Chem. 93 (2015) 93–100.

[27] R. Quiroga, M.A. Villarreal, Vinardo: a scoring function based on autodock vina improves scoring, docking, and virtual screening, PLoS One 11 (2016) e0155183.

[28] Freely available under the GNU Public License v2.0 from < http://smina.sf.net > (last access 12/13/2017).

[29] R. Salomon-Ferrer, A.W. Goetz, D. Poole, S. Le Grand, R.C. Walker, Routine microsecond molecular dynamics simulations with AMBER - Part II: particle mesh Ewald, J. Chem. Theory Comput. 9 (2013) 3878–3888.

[30] S. Le Grand, A.W. Goetz, R.C. Walker, SPFP: Speed without compromise - a mixed precision model for GPU accelerated molecular dynamics simulations, Comp. Phys. Comm. 184 (2013) 374–380.

[31] W. Humphrey, A. Dalke, K. Schulten, VMD - visual molecular dynamics, J. Mol. Graphics. 14 (1996) 33–38.

[32] Maestro Version 10.6.014, MMshare Version 3.4.014, Release 2016-2, Platform Darwin-x86_64. Maestro, Schrödinger, LLC, New York, NY, 2016.

[33] P. Li, K.M. Merz Jr., MCPB.py: a python based Metal Center Parameter Builder, J. Chem. Inf. Model. 56 (2016) 599–604.

[34] P. Li, L.F. Song, K.M. Merz Jr., Systematic parameterization of monovalent ions employing the nonbonded model, J. Chem. Theory Comput. 11 (2015) 1645–1657.

[35] M.F. Lucas, E. Monza, L.J. Jorgensen, H.A. Ernst, K. Piontek, M.J. Bjerrum, A.T. Martinez, S. Camarero, V. Guallar, Simulating substrate recognition and oxidation in laccases: from description to design, J. Chem. Theory Comput. 13 (2017) 1462–1467.

[36] S. Acebes, E. Fernandez-Fueyo, E. Monza, M.F. Lucas, D. Almendral, F.J. Ruiz-Dueñas, H. Lund, A.T. Martinez, V. Guallar, Rational enzyme engineering through biophysical and biochemical modeling, ACS Catal. 6 (2016) 1624–1629.

[37] B. Deri, M. Kanteev, M. Goldfeder, D. Lecina, V. Guallar, N. Adir, A. Fishman, The unravelling of the complex pattern of tyrosinase inhibition, Sci. Rep. 6 (2016) 34993.

[38] J.A. Maier, C. Martinez, K. Kasavajhala, L. Wickstrom, K.E. Hauser, C. Simmerling, Ff14sb: improving the accuracy of protein side chain and backbone parameters from Ff99sb, J. Chem. Theory Comput. 11 (2015) 3696–3713.

[39] J. Wang, W. Wang, P.A. Kollman, D.A. Case, Automatic atom type and bond type perception in molecular mechanical calculations, J. Mol. Graph. Model. 25 (2006) 247–260.

[40] C.I. Bayly, P. Cieplak, W. Cornell, P.A. Kollman, A well-behaved electrostatic potential based method using charge restraints for deriving atomic charges: the resp. model, J. Phys. Chem. 97 (1993) 10269–10280.

[41] A. Onufriev, D. Bashford, D.A. Case, Exploring protein native states and large-scale conformational changes with a modified generalized born model, Proteins 55 (2004) 383–394.